Single-State Measurement of Electrical Conductivity of Warm Dense Gold

K. Widmann,[1] T. Ao,[2] M. E. Foord,[1] D. F. Price,[1] A. D. Ellis,[1] P. T. Springer,[1] and A. Ng[1,2]

[1]*Department of Physics and Advanced Technologies, Lawrence Livermore National Laboratory, Livermore, California 94551, USA*
[2]*Department of Physics & Astronomy, University of British Columbia, Vancouver, B.C., Canada*

(Received 8 September 2003; published 25 March 2004)

We report on a single-state measurement of electrical conductivity of warm dense gold in the solid to plasma transition regime. This is achieved using the idealized slab plasma approach of isochoric heating of ultrathin samples by a femtosecond laser, coupled with femtosecond probe measurements of reflectivity and transmission. The experiment also reveals the time scale associated with the disassembly of laser heated solid.

DOI: 10.1103/PhysRevLett.92.125002 PACS numbers: 52.50.Jm, 52.25.Fi, 52.25.Os, 52.38.–r

There has been a long-standing interest in the electrical conductivity of warm dense matter (states with comparable thermal and Fermi energies) in which the ions are strongly correlated and the electrons are degenerate. On the one hand, this is driven by the practical need of ac conductivity for the simulation of laser-matter interaction and high energy density pulse power phenomena as well as the use of dc conductivity as a surrogate measure of electron thermal conductivity via the Wiedemann-Franz law. On the other hand, there is the fundamental desire to understand charged particle transport in the difficult regime of solid to plasma transition.

The first dense plasma conductivity model of Lee and More [1] is a semiclassical treatment based on the Boltzmann transport equation in relaxation time approximation and a Coulomb cross section legislated by a cutoff in the strong coupling regime. The model has provided the much-needed global data over a wide parameter space. Another global conductivity model is a quantum mechanical treatment due to Rinker [2] who describes the electron-ion interaction in an atom-in-jellium approach and evaluates the electrical conductivity using the Ziman formulation. The first experiment to test these models in the strongly coupled plasma regime was the measurement of optical reflectivity of shock released aluminum [3]. The results corroborated predictions derived from simulations using Lee and More conductivity and a Sesame equation of state [4]. Using measurements of the reflectivity of a femtosecond-laser pulse by aluminum, Milchberg *et al.* [5] later deduced values of dc resistivity as a function of electron temperature by assuming a constant electron density gradient and uniform electron temperature. The data appear to deviate substantially from the Lee and More and the Rinker models [1,2] as well as those based on the treatment of collision operator [6] and density-functional theory [7]. However, when time-dependent gradient effects in the heated plasma are taken into account [8], the data of Milchberg *et al.* were found to be reasonably consistent with results of simulations when either the Lee and More or the density-functional-theory conductivity model was used in conjunction with a Sesame equation of state [4]. This clearly underlines the intrinsic difficulty of testing theory with integral measurements on nonuniform systems consisting of multiple states. It also heightens the need for single-state data to allow a direct test of theory.

The task of obtaining data on single, warm dense matter state is challenging. At pressures reaching 10^6 atmospheres and above, such a state expands rapidly into its surroundings and cannot be confined readily by external means. To meet this challenge, Forsman *et al.* put forth the idealized slab plasma approach [9] based on the isochoric heating of an ultrathin sample by an intense, femtosecond laser. They also elucidated the means of obtaining ac conductivity directly from reflectivity and transmission measurements using a pump-probe technique. In this Letter, we present the long awaited experimental realization of such ideas to obtain single-state electrical conductivity data of gold through the solid to plasma transition.

Figure 1 shows a schematic of the experimental setup. Free-standing gold foils with thicknesses ranging from 280–320 Å are heated by a 400 nm, 150 fs (FWHM) pump laser that is focused with $f/50$ optics to produce a focal spot diameter of 65 μm (FWHM) with a

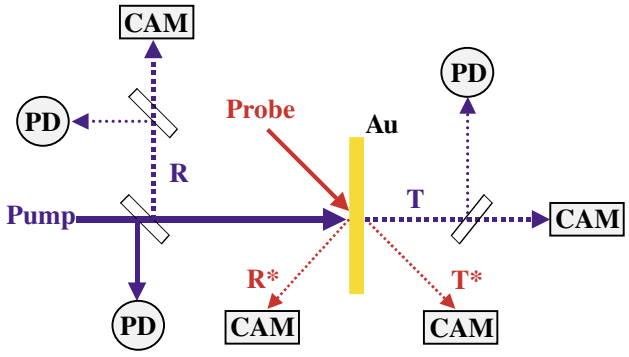

FIG. 1 (color online). Schematic of the experimental setup. Laser-pulse energies are measured with photodiodes (PD) which are attached to integrating spheres. Images are recorded with CCTV cameras (CAM) [10].

maximum irradiance of about 10^{13} W/cm^2 and a main-to-prepulse contrast better than 10^7. The reflectivity R and transmission T of the pump laser are monitored with $f/8$ optics and recorded by photodiodes and CCTV cameras (CAM) [10] (8 μm resolution) to yield pump absorption. To determine the optical property of the heated foil, we use a collimated 800 nm, 150 fs (FWHM) probe laser with a beam diameter of 650 μm at 45° incidence. The reflectivity R^* and transmission T^* of the probe are monitored with $f/3$ optics and recorded by CCTV cameras (CAM, 3 μm resolution) [10]. The signals from the heated region are compared *in situ* with those from the unheated region of the foil. The latter values are absolutely calibrated.

Gold is chosen for this study because it is an inert metal and its available purity of 99.99%. The 280–320 Å thick samples of normal solid density (19.3 g/cm^3) are obtained commercially [11]. The foils are floated onto stainless steel support plates with circular openings of 600 μm in diameter. The flatness of the foil over the opening is determined by interferometric measurements at 632.8 nm to be better than $\lambda/10$ over a region of 300 μm diameter. The supplied values of density and thickness of each foil are corroborated by *in situ* reflectivity and transmission measurements using the 800 nm probe laser.

The absorbed energy density of the heated foil is determined directly from spatially resolved measurements of the reflectivity and transmission of the pump laser. Although the thickness of the foil exceeds the skin depth for the pump laser, thermal conduction renders near uniform energy deposition in the sample. For a Fermi speed of 1.4×10^8 cm/s, the mean free path of conduction electrons is $\approx$ 390 Å in gold at normal conditions and the transit time through a 320 Å foil is $\approx$ 23 fs.

Figures 2(a) and 2(b) show an example of the temporal behavior of the reflectivity and transmission of a heated, 280 $\pm$ 10 Å foil for the 800 nm, *S*-polarized probe laser. *S* polarization is better suited to the idealized slab plasma approach being free from the complexity of resonant absorption [12]. The data correspond to measurements taken from the central, 20 μm diameter region of the pump laser spot for an increase in energy density due to pump absorption of $\Delta\varepsilon = 4.8 \times 10^6$ J/kg. The temporal resolution of the measurement is determined by the duration of the probe pulse. Zero time delay is taken arbitrarily to be the onset of observable changes in the reflectivity and transmission signals. Both signals show an initial rapid change in $\leq$ 1 ps. This is followed by a quasi-steady-state phase that lasts for about 4 ps before rapid changes appear again. Similar temporal behavior is observed for $\Delta\varepsilon$ up to 2×10^7 J/kg.

Since the pump pulse has a FWHM of 150 fs and a base width of 600 fs (1% peak intensity), the initial rapid change in probe reflectivity and transmission can be attributed to the heating process. The end of laser heating

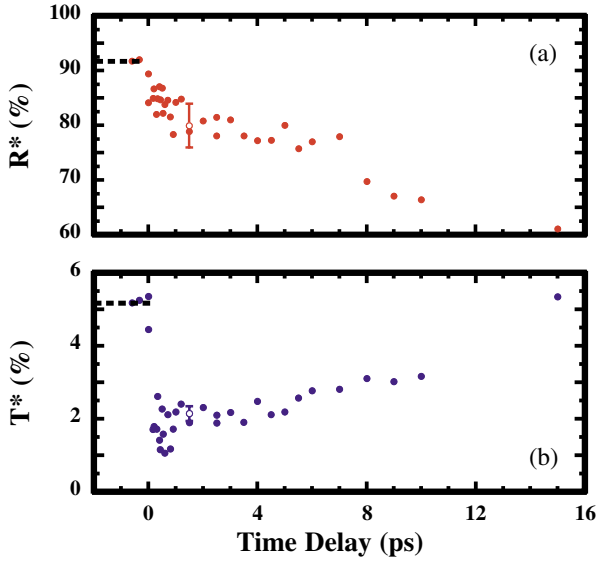

FIG. 2 (color online). Temporal behaviors of the probe reflectivity (a) and transmission (b) for an increase in energy density of 4.8×10^6 J/kg. Representative error bars are shown.

is identified by the start of the quasi-steady-state behavior in the observed optical properties. This corresponds to a time delay of 1.5 ps in Fig. 2. At such an early time, hydrodynamic expansion governed by the motion of ions is not expected to be significant and the idealized slab plasma approximation should apply. Thus, the observed probe reflectivity and transmission can be used to solve the Helmholtz equations for the real and imaginary parts of the ac conductivity σ_ω for a single, well-defined state $(\rho_0, \Delta\varepsilon)$ of the heated foil. Figure 3 shows our results for different energy densities. It should be noted that $\Delta\varepsilon$

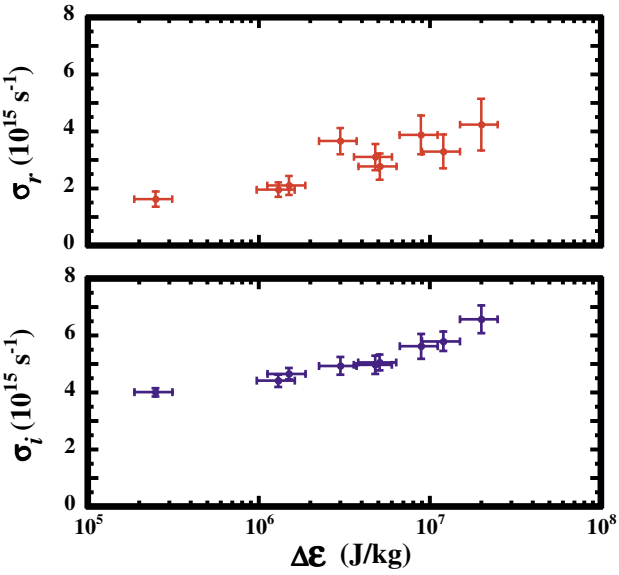

FIG. 3 (color online). The real and imaginary parts of the ac conductivity as a function of increase in energy density.

constrains only the total energy density distributed among electrons, ions, and ionization. Earlier measurements on femtosecond-laser heating of gold have revealed electron-lattice equilibration times of 2–3 ps [13]. This suggests that at the end of the pump pulse the ion temperature remains negligible compared with the electron temperature.

While the data set of $\sigma_\omega(\rho_0, \Delta\varepsilon)$ in Fig. 3 presents a new opportunity to test equation of state and transport theories in the solid to plasma transition regime particularly in view of the recent development in quantum molecular dynamics approaches [14], such a coordinated effort is beyond the scope of this study. Nonetheless, it is instructional to examine the implications of the results by assuming nearly free electron behavior of warm dense gold. This assumption may be justified given (i) the absence of interband transitions at 800 nm at normal condition, (ii) the likely excitation of perhaps only one $5d$ electron at the highest energy density considered, and (iii) that electrical conductivity is effected by conduction electrons near the Fermi surface. Accordingly, the ac conductivity can be described by the Drude model [15] as $\sigma_\omega = \sigma_r + i\sigma_i = \sigma_0(1 + i\omega\tau)/(1 + \omega^2\tau^2)$. The collision time τ is then given by the measured ratio of the imaginary to the real part, σ_i/σ_r. This further allows an evaluation of the dc conductivity σ_0, using σ_i or σ_r as well as the electron density n_e from $\sigma_0 = n_e e^2\tau/m_e$ where m_e is the electron mass. The results (Fig. 4) appear to follow general expectations that τ and σ_0 are less than their values at normal conditions, while the average ionization increases approximately from the normal condition value of 1 ($\tau = 2.8 \times 10^{-14}\,\mathrm{s}^{-1}$ [16] and $n_e = 5.9 \times 10^{22}\,\mathrm{cm}^{-3}$ at $\Delta\varepsilon = 0$). These offer a further check on theory. It is interesting to note that our dc conductivity values ($\sigma_0 = 1.3 \times 10^{16}\,\mathrm{s}^{-1} \approx 1.4 \times 10^6\,\mathrm{S/m}$) appear to lie along the solid-density extrapolation of dc conductivities of expanded metals measured by Kloss *et al.* [17], DeSilva and Katsouros [18], and Saleem *et al.* [19].

The relatively long-lived quasi-steady-state phase seen from probe reflectivity and transmission in Fig. 2 is intriguing. Its duration, τ_{QS}, is found to decrease with increase in energy density as shown in Fig. 5. When a solid is irradiated with an intense femtosecond laser, only the electrons gain energy while the lattice remains cold because of the relatively slow equilibration rate between the two components. While the electrons tend to escape from the target, such a process is self-regulated by the space charge field. This leads to the formation of an electron plasma sheath on the surface of the foil. For the S-polarized, 800 nm probe, the relevant region of the sheath is that extending to the critical density of $n_e = 1.6 \times 10^{21}\,\mathrm{cm}^{-3}$. Even for temperatures of 10 eV, the extent of such a region is extremely small since the associated Debye length is about 6 Å. This would suggest that the electron plasma sheath is a negligible perturbation for the probe. It also suggests that the formation of

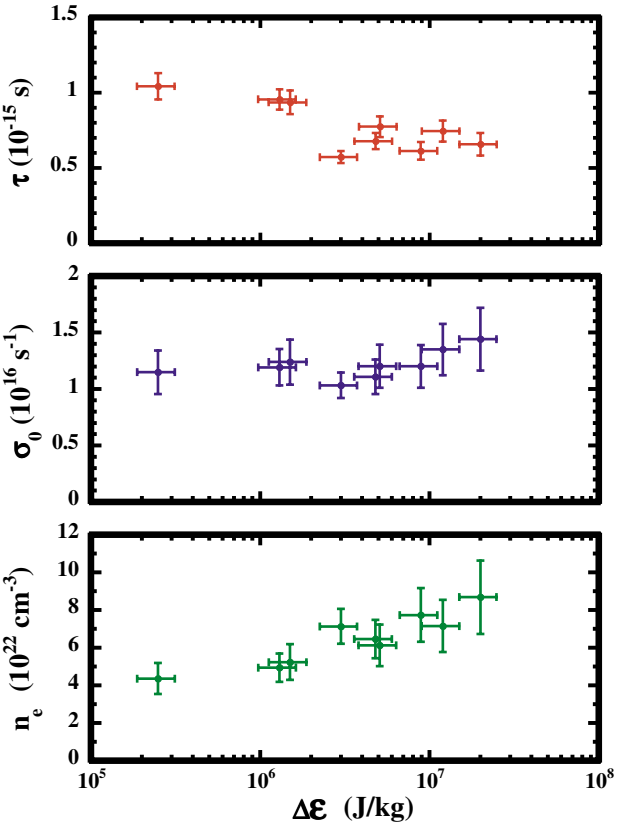

FIG. 4 (color online). Values of collision time, dc conductivity, and electron density as a function of increase in energy density.

the sheath can be extremely fast. On the other hand, melting of the lattice will occur when it acquires sufficient energy from the electrons. Only then can hydrodynamic expansion start to cause disassembly of the foil. This will give rise to a rapid change in probe reflectivity and transmission as seen in late times in Fig. 2. The quasi-steady-state phase is thus interpreted as that occurring prior to foil disassembly since once hydrodynamic expansion is initiated, it is unlikely that continual increases in the electron density gradient scale length can

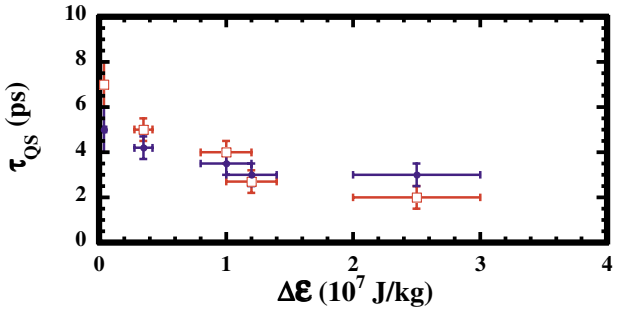

FIG. 5 (color online). Duration of the quasi-steady-state phase, τ_{QS}, as a function of increase in energy density as seen from reflectivity (square) and transmission (circle) measurements.

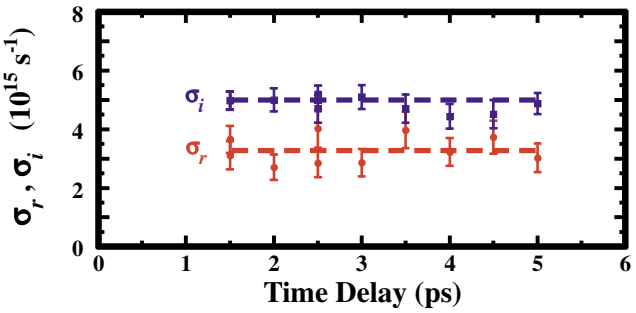

FIG. 6 (color online). The real and imaginary parts of the ac conductivity during the quasi-steady-state phase for the data presented in Fig. 2. The dashed lines show the linear best fit to the data.

be compensated exactly, at every instant, with changes in the plasma conductivity to produce constant reflectivity and transmission signals. This supports our earlier assertion of insignificant hydrodynamic expansion at the end of the pump pulse. We are also led to conjecture that the duration of the quasi-steady-state phase (Fig. 5) is a measure of the time scale associated with the disassembly of the heated solid. This is influenced by both the rate of energy exchange between electrons and the lattice and the nonequilibrium melting process. Our observation can thus provide an interesting test of quantum molecular dynamics simulations for such a transition. Equally important, it also suggests that meaningful measurements of the properties of the idealized slab plasma state can be made with ps resolution. This greatly broadens the availability of suitable probes and hence the variety of physical properties that can be studied.

The apparent lack of significant hydrodynamic expansion during the quasi-steady phase further allows us to extend the idealized slab plasma approach of using the probe reflectivity and transmission in the Helmholtz equations to determine the real and imaginary parts of the ac conductivity σ_ω. As an example, Fig. 6 shows the results corresponding to the data shown in Fig. 2. In such a quasi-steady-state phase, while the macroscopic state remains unchanged as characterized by $\rho_0 = 19.3$ g/cm^3 and $\Delta\varepsilon = 4.8 \times 10^6$ J/kg, the microscopic state is changing in time, albeit slowly, as electrons exchange energy with ions. The essentially constant conductivity values shown in Fig. 6 are thus indicative of a weak dependence on electron and ion temperatures in the observed regime.

In conclusion, we have presented results that demonstrate the idealized slab plasma approach [9] in determining the ac conductivity of warm dense gold. The single-state data that extend over the solid to plasma transition region can be used to test equation of state and transport theories on nonequilibrium systems. The assumption of nearly free electron behavior provides further insights into the collision time and dc conductivity as well as electron density for an assessment of ionization physics. Our observation has also revealed the time scale associated with the disassembly of a femtosecond-laser heated solid.

This work was performed under the auspices of the U.S. Department of Energy by University of California Lawrence Livermore National Laboratory under Contract No. W-7405-ENG-48 and supported by the Natural Sciences & Engineering Research Council of Canada.

[1] Y. T. Lee and R. M. More, Phys. Fluids **27**, 1273 (1984).
[2] G. A. Rinker, Phys. Rev. B **31**, 4207 (1985); **31**, 4220 (1985).
[3] A. Ng *et al.*, Phys. Rev. Lett. **57**, 1595 (1986).
[4] K. S. Holian, Los Alamos National Laboratory Report No. LA–10160–MS UC–34, 1984 (unpublished).
[5] H. M. Milchberg *et al.*, Phys. Rev. Lett. **61**, 2364 (1988).
[6] R. Cauble *et al.*, in *Femtosecond to Nanosecond High Intensity Lasers and Applications*, SPIE Proceedings Vol. 1229 (SPIE–International Society for Optical Engineering, Bellingham, WA, 1990), p. 221.
[7] M. W. C. Dharma-wardana and F. Perrot, Phys. Lett. A **163**, 223 (1992).
[8] A. Ng *et al.*, Phys. Rev. Lett. **72**, 3351 (1994).
[9] A. Forsman *et al.*, Phys. Rev. E **58**, R1248 (1998).
[10] Hitachi Denshi CCTV cameras (KP-101A, KP-140U) and Coreco Viper-Quad frame grabber.
[11] Schafer Corp., Livermore, CA 94550, U.S.A.
[12] V. L. Ginzburg, *The Propagation of Electromagnetic Waves in Plasmas* (Pergamon, New York, 1970), p. 260.
[13] R. W. Schoenlein *et al.*, Phys. Rev. Lett. **58**, 1680 (1987).
[14] M. P. Desjarlais *et al.*, Phys. Rev. E **66**, 025401 (2002).
[15] P. Drude, Ann. Phys. (Leipzig) **1**, 566 (1900).
[16] G. T. Meaden, *Electrical Resistance of Metals* (Plenum, New York, 1965).
[17] A. Kloss, T. Motzke, R. Grossjohann, and H. Hess, Phys. Rev. E **54**, 5851 (1996).
[18] A. W. DeSilva and J. D. Katsouros, J. Phys. IV (France) **10**, 209 (2000).
[19] S. Saleem, J. Haun, and H.-J. Kunze, Phys. Rev. E **64**, 056403 (2001).